ELSEVIER

Thermochimica Acta 319 (1998) 139–149

thermochimica acta

A kinetic study of the thermal decomposition of polyesters by controlled-rate thermogravimetry

Tadashi Arii[a,*], Shoji Ichihara[b], Hideaki Nakagawa[b], Nobuyuki Fujii[c]

[a] *Thermal Analysis Division, RIGAKU Corporation, 3-9-12 Matubara, Akishima, Tokyo 196, Japan*
[b] *Materials Characterization and Analysis Lab., Mitsubishi Chemical Co. 8-3-1, Chu-ou, Ami-cho, Ibaraki 300-03, Japan*
[c] *Department of Chemistry, Nagaoka University of Technology, 1603-1 Kamitomioka, Nagaoka, Niigata 940-21, Japan*

Received 12 August 1997; accepted 1 June 1998

Abstract

A kinetic study of the thermal decomposition of engineering polyesters has been made by means of controlled-rate thermogravimetry (CRTG), a procedure that is a part of controlled-rate thermal analysis (CRTA). Various decomposition rates were used in the constant decomposition rate control (CDRC) experiments, in order to estimate the apparent activation energy without prior knowledge of the actual mechanism. The kinetic equations governing the thermal decomposition of poly(ethylene terphthalate) (PET) and poly(butylene terphthalate) (PBT) were determined. The kinetic parameters of these polyesters were estimated from both, the CDRC curve and evolved-gas components, obtained from the simultaneous TG-MS system, and corresponding to a kinetic-model-supported random scission of the main chain and with $L=2$. It is concluded that analytic techniques using the thermogravimetric traces obtained from different decomposition rates at CDRC are capable of establishing unique kinetic parameters. CRTG (CRTA) offers significant advantages in this field of study when dealing with thermal decomposition of polymers. © 1998 Elsevier Science B.V.

Keywords: Kinetics; Controlled-rate thermal analysis (CRTA); Constant decomposition rate control (CDRC); Thermal decomposition; Polyester; TG-MS; Reaction model

1. Introduction

Both thermogravimetry (TG) and differential thermal analysis (DTA) are widely used to investigate the thermal decomposition of polymers and to assess their relative thermal stabilities. Also, considerable attention has been directed toward the exploitation of thermogravimetric data at different heating rates for the determination of kinetic parameters such as activation energy, pre-exponential factor and reaction mechanism. Thus, many kinetic methods make two assumptions, (i) that these parameters are useful in characterizing a particular polymer degradation, and (ii) that the thermogram for each particular set of these parameters is unique. However, the method has not been applied widely, presumably because it needs a knowledge of conversion as well as the rate of conversion.

In recent years, the determination of, kinetic parameters by non-isothermal methods has been used extensively as this method has several advantages over isothermal methods. With non-isothermal methods, however, because of temperature dependence of the reaction rate, the analytical treatment of data

*Corresponding author.

PII S0040-6031(98)00414-6

generally becomes complex. An underestimation and/or overestimation of these kinetic effects may result from an incomplete understanding of the kinetics of the solid state reactions.

With conventional thermal analysis (TA), the temperature of the sample follows some predetermined program as a function of time. On the other hand, with the new approaches proposed, namely controlled transformation rate thermal analysis [1,2], stepwise isothermal analysis [3] and the quasi-isothermal and quasi-isobaric method [4], some parameters follow a predetermined program as functions of time, this being achieved by adjusting the sample temperature. These techniques maintain a constant reaction rate, and control the pressure of the evolved species in the reaction environment. CRTA is, therefore, characterized by the fact that it does not require the predetermined temperature programs that are indispensable for TA. In the previous articles, the authors have demonstrated that CRTA represents a new approach for thermal analysis that offers significant advantages over conventional methods [5–8]. Especially, it gives improved sensitivity and resolution of the thermal analysis curve.

With the present CRTG method, uniform conditions are maintained throughout the sample by means of an appropriate control of the reaction rate. Consequently, it is to be preferred for measuring kinetic parameters.

On the other hand, papers dealing with model chemical reactions in kinetic studies are scarce, although this is possibly the field in which CRTA is most novel and powerful. Therefore, the CRTA appears to be an excellent technique for the study of degradation reactions.

It is the purpose of this paper to determine the reaction mechanism and kinetic parameters in order to confirm the suitability of this approach for kinetic analysis of the thermal decomposition of polyesters.

2. Experimental

2.1. Material

Samples of poly(ethylene terphthalate) (PET) and poly(butylene terphthalate) (PBT) used in this study were supplied by Mitsubishi as commercial material. The samples (ca. 1–15 mg) were heated in an open cylindrical platinum crucible of 5 mm diameter and 2.5 mm height, in an inert helium/nitrogen atmosphere and a flow rate of 200 $cm^3 min^{-1}$.

A Rigaku Thermo Plus TG-DTA 8120D thermogravimetry– differential thermal analyzer, upgraded with a dynamic TG-DTA module, was used to measure the mass profile. At the present constant decomposition rate control (CDRC), in which control of the heating/cooling rate of the sample is dependent on the rate of loss of sample mass. Thus, the experiments were all carried out with fully automated and computerized controlled rate thermogravimeric (CRTG) equipment, which has been previously described [9–13], and operates between 300 and 1000 K. The decomposition rate was kept constant at any value from 0.1 to 0.6% min^{-1}.

In case of PBT, CDRC was initiated when the sample temperature reached 643 K, where the normal temperature program of 5 K min^{-1} was carried out. This switchover point from temperature to mass control was selected in the range of the onset of decomposition, which was determined from a prior TG experiment.

The dynamic TG-DTA was connected to a Hewlett-Packard 5890II-5971A gas chromatography – quadrupole mass spectrometer (GC-MS), using a Rigaku TG-MS interface to create an integrated simultaneous TG-DTA/GC-MS system.

This original TG-DTA/GC-MS system can be used for two kinds of interface modes. They are distinguished between continuous sampling (direct coupling mode), in which a purge gas stream is continuously recorded with a TG-DTA signal as a function of time or temperature for ‘on-line’ analysis, and intermittent sampling (trap coupling mode), in which a portion of the evolved gases is collected over a selected temperature range and then analyzed as ‘off-line’ GC-MS. On the direct coupling mode, the thermograms obtained were then combined with the mass spectrometer total ion chromatogram (TIC) to allow the simultaneous identification of the evolved gases as a function of mass loss. A library search was a procedure that compared the spectrum of an unknown compound against a library of reference spectra, using NIST/EPA/NIH chemical structures database. The instrumentation has been described in more detail elsewhere [10,13].

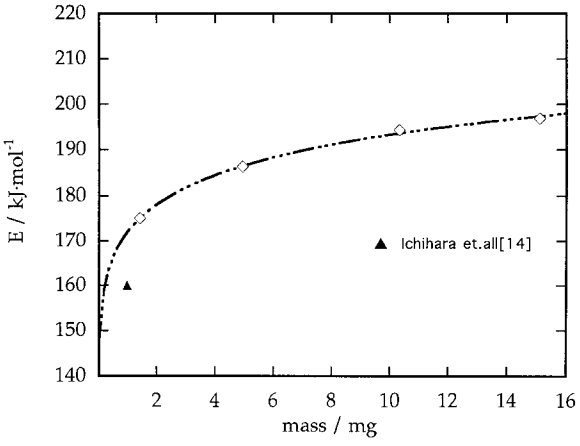

Fig. 1. Mass dependence of apparent activation energy for the thermal decomposition of PBT. Results were analyzed by using the isoconversion method of Ozawa [15].

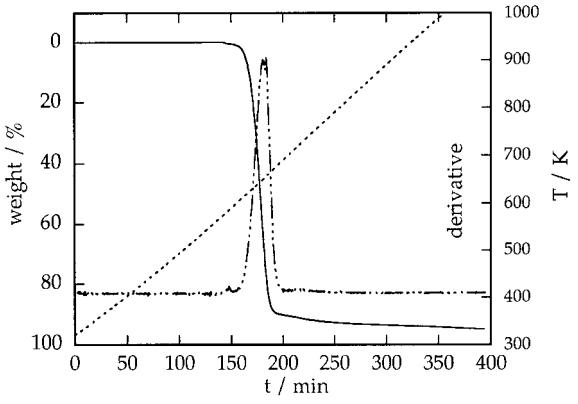

Fig. 2. Experimental TG curves at a ramping rate 5°C min^{-1} for thermal decomposition of PBT. (———) Weight; (- - -) temperature; (— - - -) derivative.

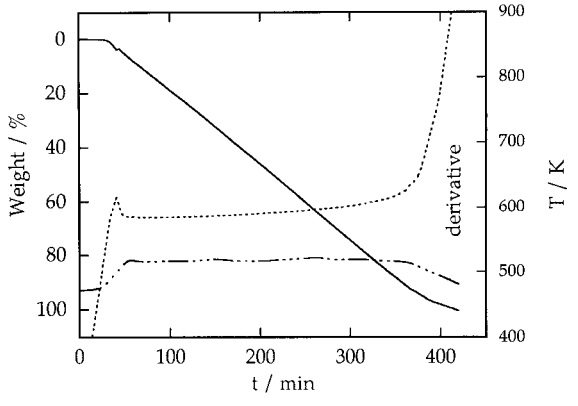

Fig. 3. Experimental CDRC curves for the thermal decomposition of PBT. (———) Weight; (- - -) temperature; (— - - -) derivative.

3. Results and discussion

In previous publications, it was established that the preferred initial weight was ca. 1 mg, to analyze the thermal decomposition behaviors of polymers using the results of TG with conventional TA in which the heating rate was set up between 1 and 10 K min^{-1}[14]. However, care must be taken to select the correct method to obtain meaningful kinetic parameters. The thermal conductivity of the polymeric material is generally low, so that, with linear heating rate experiments, there are special problems of pressure and temperature gradients within the sample. Fig. 1 is a good illustration of the dependence of the apparent activation energy for the thermal decomposition of PBT sample on sample mass. The apparent activation energy decreases steeply with decreasing initial weight of sample. On the other hand, if the sample mass is too small the mass loss (and mass loss rate) signal becomes noisy and the estimation of activation energy gives inaccurate values.

Figs. 2 and 3 show both, the % mass loss with temperature for the decomposition of PBT obtained by conventional TG at 5 K min^{-1} and the CRTG (CDRC) method. The sample is gradually, and continuously, decomposing between 550 and 800 K under conventional TA condition. The effect of applying the CDRC techniques is to produce significant decomposition steps at low temperatures and over narrower temperature ranges than conventional TA. This is a major reason that the CRTA technique brings about a mass loss curve with high resolution.

There is also a characteristic decomposition curve obtained by means of the CDRC method in Fig. 3. The mass-loss profile has a unique shape which reflects the difference in the decomposition mechanism directly, and the kinetic analysis can be easily adapted under this CDRC condition, as discussed below.

If it is assumed that the isothermal rate of conversion, $d\alpha/dt$, is a linear function of a single temperature-dependent rate constant, k, and some temperature-independent function of the conversion,

α, i.e.

$$d\alpha/dt = kf(\alpha) \quad (1)$$

Here, α, the degree of completion (or advancement, extent of reaction) is defined as the conversion with respect to initial weight of material. Thus, $\alpha=1-(W/W_0)$, where W_0 and W are the initial and actual sample masses, respectively, $f(\alpha)$ a function depending on the kinetic model obeyed by the reaction, and the rate constant k is frequently assumed to obey the Arrhenius relationship

$$k = A\exp(-E/RT) \quad (2)$$

where A is the pre-exponential factor, E the apparent activation energy, R the gas constant and T the absolute temperature. Normally several kinetic functions can be derived by simply assuming mechanistic models of the solid-state reactions. However, with random scission of the main chain of the polymer, the measured quantity in thermal analysis is not necessarily equal or proportional to the amount of the reacting species or the reacting chemical structure, so that the conversion, α, measured by thermal analysis is a function of the amount of the reacting species or the reacting structure, x, as follow:

$$\alpha = f(x) \quad (3)$$

The reaction proceeds in accordance with the usual kinetic formula:

$$dx/dt = A\exp(-E/RT)g(x) \quad (4)$$

Scission of the main chain of a polymer can be classified into random scission (RSL) and depolymerization (Fn). For example, if depolymerization is initiated at chain ends and the zip length of the depropagation reaction is much shorter than the polymeric main length, as is the case in high molecular weight poly(methyl methacrylate) (PMMA), then a large portion of the reaction follows zero-order kinetics. If the zip length is much larger than the polymer chain length, then first-order kinetics results [16]. However, random scission of the main chain of a polymer is different to that of any other reaction mechanism which can be described as $\alpha=f(x)=x$.

The scission of bonds proceeds by first-order kinetics. The molecular weight decreases, finally producing a statistical distribution. The scission portion occurs randomly and, therefore, the molecules decompose producing evaporates of low molecular weights. The reaction proceeds according to the following equation [17]:

$$X = 1-\alpha = (1-x)^{L-1}[1 + x(N-L)(L-1)/N] \quad (5)$$

where, $N-1$ is the initial number of carbon atoms in the chain skeleton, L the number of carbon atoms in the smallest chain that does not evaporate, and, here, x the fraction of bonds broken. Eliminating N from Eq. (5) for the simplest case, $N \gg L$, results in

$$X(1-x)^{L-1}[1 + x(L-1)] \quad (6)$$

The CDRC method, with constant acceleration of the mass loss, proposed in this study implies that the mass-loss profile is kept as a linear function of time, i.e. $d\alpha/dt=C$ (constant), then Eq. (6) and $dx/dt=k(1-x)$ can be derived:

$$d\alpha/dt \equiv (d\alpha/dx)(dx)/dt) = -dX/dt \equiv -(dX/dx)(dx/dt) \quad (7)$$

$$dX/dx = -L(L-1)x(1-x)^{L-2} \quad (8)$$

$$d\alpha/dt = C = -dX/dt = kL(L-1)x(1-x)^{L-1} \equiv A\exp(-E/RT)g(X) \quad (9)$$

After taking logarithms, This leads to:

$$\ln(g(X)) = E/RT - \ln(A/C) \quad (10)$$

Thus, assuming that the term $\ln(A/C)$ is a constant and plots of $\ln(g(X))$ vs. reciprocal of temperature, $1/T$, for various functions g(X) should be linear, having a slope E/R. This indicates that it is possible to obtain the activation energy from one single CDRC experiment. In addition, it follows that the general shape of the experimental curve, X vs. T, obtained at a constant reaction rate is in itself quite meaningful for the selection of the actual mechanism. This is demonstrated in Fig. 4, which shows theoretical curves calculated by assuming the respective kinetic models involving the first-order (F1), second-order (F2) reactions and random scission in the main chain at $L=2$ (RS2) and $L=3$ (RS3) in Eq. (9) and the following kinetic parameters: $E=160\ \mathrm{kJ\ mol^{-1}}$, $A=2.0\times 1012\ \mathrm{min^{-1}}$ and $C=4.0\times10^{-3}\ \mathrm{min^{-1}}$. In particular, the kinetic model of the RSL type leads to a curve with a temperature minimum. This profile has impor-

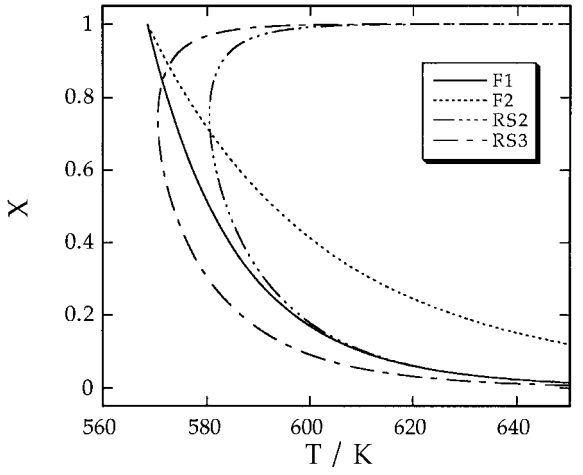

Fig. 4. Shape of the theoretical CRTA curves corresponding to the kinetic models obtained assuming E=160 kJ mol^{-1}, A=2×10^{12} min^{-1} and C=4×10^{-3} min^{-1}.

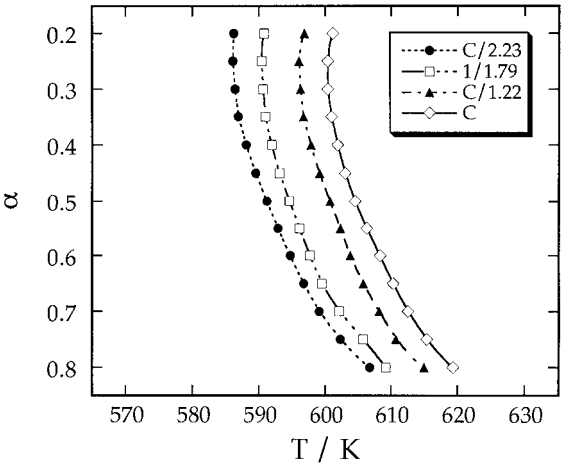

Fig. 5. Experimental α vs. T plots obtained by using different decomposition rates for the thermal decomposition of PBT.

tant information in the elucidation of this scheme of kinetics for thermal decomposition, since it can be used as the master curve for comparison with experimental data. The shape of the experimental profile shown in Fig. 3 may be attributed to the kinetic model of the RSL type, and is in agreement with that obtained from previous TG analysis carried out using a small-sized sample [14].

Fig. 5 shows the α vs. T plot obtained by using four different decomposition rates of relative values C, C/1.22, C/1.79 and C/2.23, respectively. The circles indicate the T at $\Delta\alpha$=0.05 increments over the $0.2 \leq \alpha \leq 0.8$ range. These plots imply that when a molecule of this material reaches a molecular size which allowed groups to evaporate on bond scission, the temperature begins to drop gradually as the reaction proceeds at the pre-selected rate. Fig. 6 shows the results obtained from representation of Eq. (10) at a decomposition rate, C/1.79, using the kinetic model of F1, F2, RS2 and RS3, respectively. Also, Table 1 shows the results calculated for each decomposition rate. From the RSL kinetics, we can see that a slight increase in the correlation coefficients was observed as compared to the case where the Fn kinetics was used. In the case of Fn type, however, it is clear that the difference between the experimental data and theoretical curve is greater with increasing reciprocal temperatures, 1000/T.

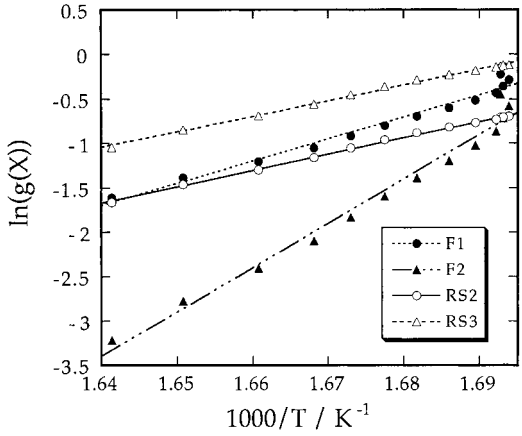

Fig. 6. Results obtained from the representation of Eq. (10) by assuming the kinetic models of the Fn and RSL types in a single CDRC experiment.

Nevertheless, the obtained correlation coefficients predominate in case of RS2 and RS3 and are not significantly different. Moreover, the kinetic parameters estimated from each decomposition rate contain a large dispersion. We should notice that, just because the correlation coefficients are close to 1.0, it does not follow that the mechanism can be unambiguously selected on the basis of these representations. This means that the difference in behaviour of similar models within a group is small, and it would be

Table 1
Results obtained from the representation of [10] at four different decomposition rates for the thermal decomposition of PBT

Reaction rate	Mechanism symbol											
	F1			F2			RS2			RS3		
	r [a]	E [b]	$A\times10^{16}$ [c]	r [a]	E [b]	$A\times10^{35}$ [c]	r [a]	E [b]	$A\times10^{11}$ [c]	r [a]	E [b]	$A\times10^{10}$ [c]
C/2.23	0.9943	190	0.032	0.9942	380	0.0003	0.9970	139	12.66	0.9958	132	0.174
C/1.79	0.9894	208	1.229	0.9895	416	0.434	0.9991	153	2.362	0.9985	146	2.892
C/1.22	0.9907	215	5.070	0.9907	430	5.045	0.9971	158	6.695	0.9962	150	7.838
C	0.9889	213	3.196	0.9889	427	1.639	0.9981	157	5.496	0.9974	149	6.603
Mean	0.9908	206.5	2.382	0.9908	413.3	1.779	0.9978	151.8	6.803	0.9970	144.3	4.377
σ_n [d]		11.4	2.217		23.0	2.284		8.8	4.314		8.3	3.503

[a] Correlation coefficient.
[b] Activation energy (kJ mol^{-1}).
[c] Pre-exponential factor (min^{-1}).
[d] Standard deviation.

difficult to select unambiguously the correct mechanism. In other words, not all kinetic mechanisms can be explained by this idea. To overcome this problem, it is essential to know the nature of the decomposition products. MS technique is particularly valuable, in that it provides direct chemical information about the decomposition products. Since L is the number of carbon atoms in the smallest chain that does not evaporate, the components identified by TG-MS serve experimentally to determine the number L, (L=2, 3, 4...). The TG-MS combination method is, therefore, helpful in assessing volatilization behavior in the decomposition of polymers and providing a magnitude for L.

Fig. 7 shows a comparison of TG and DTG curves with that of the TIC curve and mass spectrum obtained at the TIC peak with maximum intensity at 685 K. Comparison of the derivative of the mass loss curve with the TIC monitored by mass spectrum clearly reveals the similarities between the two responses.

We can see that the mass fragmentation ions which are conceded as the decomposition components are within m/z=122. Fig. 8 shows the NIST mass spectra of two organic components which can be formed during thermal decomposition. By comparing the mass spectra, the m/z=77, 105, 122 ions observed are characteristic of benzoic acid, and m/z=122 is the molecular ion peak. Also, the set of m/z=27, 39, 54 ions observed simultaneously are from butadiene. In addition, these results prove that L should be taken so as to have a minimum value of two. To sum up, this analysis suggests that the RS2 kinetic model is correct. The temperature dependence of the different decomposition rates make it possible to estimate the activation energy and identify the correct

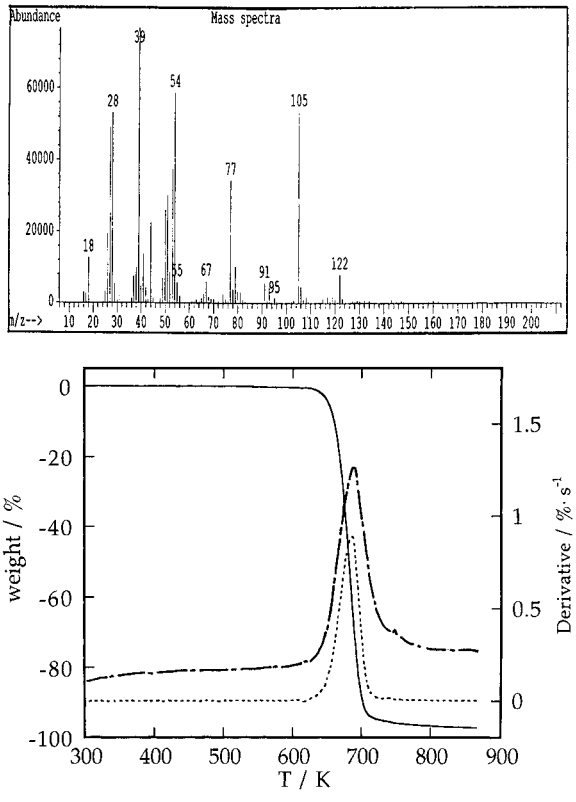

Fig. 7. Overall thermograms of TG, derivative and TIC curves for the thermal decomposition of PBT, and mass spectrum in TIC at 685 K. (———) Weight; and (- - -) derivative; (— - -) TIC.

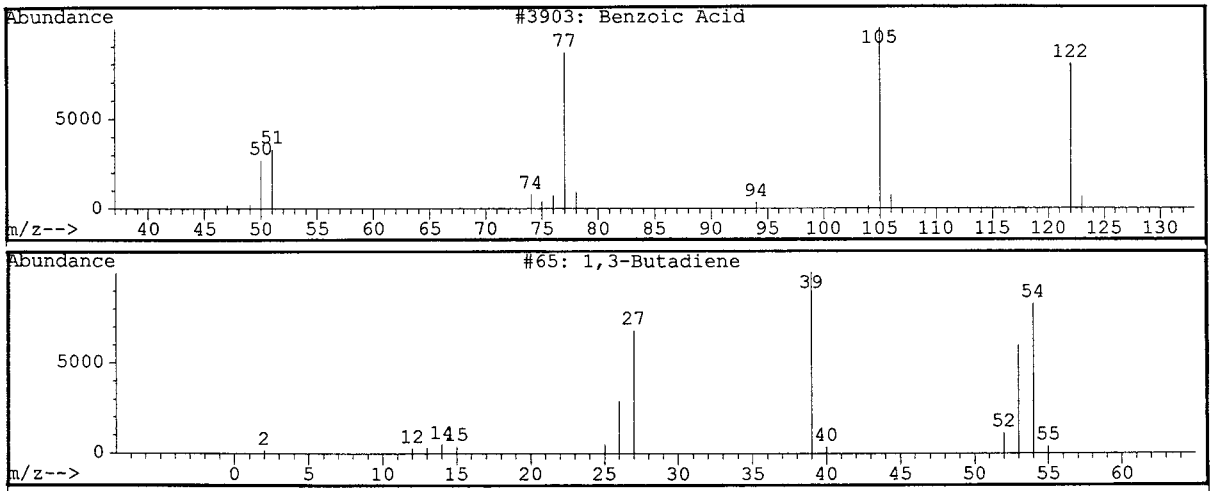

Fig. 8. Mass spectrums in the NIST database with respect to benzoic acid and butadiene, formed during the thermal decomposition of PBT.

mechanism. With two decomposition rates, Eq. (10) can be expressed as

$$\ln(C_2/C_1) = E/R(1/T_1 - 1/T_2) \quad (11)$$

where C_1 and C_2 are the two decomposition rates corresponding to temperatures T_1 and T_2, respectively.

This equation means that the activation energy can be estimated without previous knowledge of the actual reaction mechanism. Fig. 9 shows the results of analyzing each ratio of four different decomposition rates

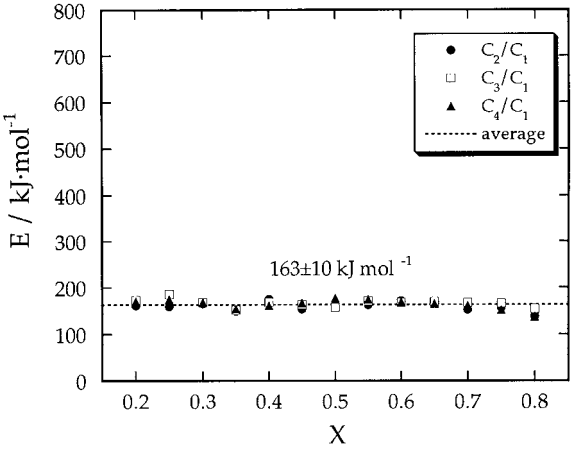

Fig. 9. Results obtained from the representation of Eq. (12) by using each ratio of four decomposition rates: C_1, C/2.23; C_2, C/1.79; C_3, C/1.22; and C_4, C.

according to Eq. (12). The mean activation energy, E, was estimated at 163 kJ mol^{-1}, and the activation energy was independent of X in the analyzed range. Moreover, it follows from the listed value of activation energy in Table 1 that the RS2 mechanism is not required.

Subsequently, an estimation of the pre-exponential factor, A, by using both, the activation energy and the kinetic model was attempted since

$$\ln(g(X)) + \ln(A) = \ln[\exp(E/RT)C] \quad (12)$$

Plots of X vs. ln [exp (E/RT)C], calculated using E=163 kJ mol^{-1} could be superposed on plots of ln ($g(X)$) by shifting the amount of ln (A) in order to coincide with the curve for the theoretical reaction model. Consequently, the kinetic model will correctly select the $g(X)$ which gave the best fit to the experimental data. Further, it has become possible to estimate the pre-exponential factor, A, from the shift.

Fig. 10 shows plots of experimental data of X vs. ln [exp (E/RT)C] at a decomposition rate of C/1.22, superposed on the X vs. ln ($g(X)$) calculated using the kinetic model F1, F2 and RS2. It is also evident from Fig. 10 that the values observed agree very closely with the RS2 model curve. The pre-exponential factors estimated are summarized in Table 2. The resulting mean pre-exponential factor, A, was estimated at 1.813×10^{12} min^{-1}. The point we wish to emphasize is

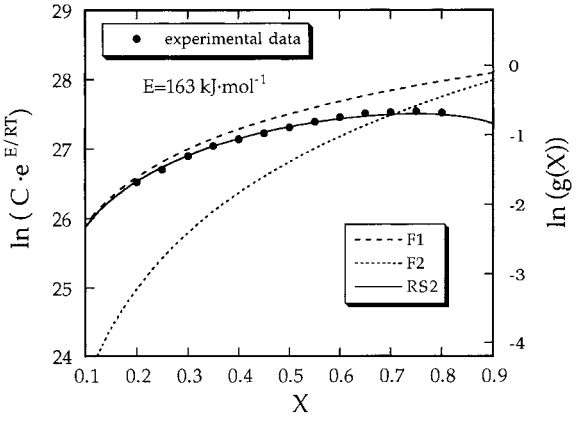

Fig. 10. Superimposition of experimental ln *C*exp (*E*/*RT*) vs. *X*, and theoretical ln (*g*(*X*)) vs. *X*. Results obtained from the representation of Eq. (12) by using a single CDRC experiment for the thermal decomposition of PBT.

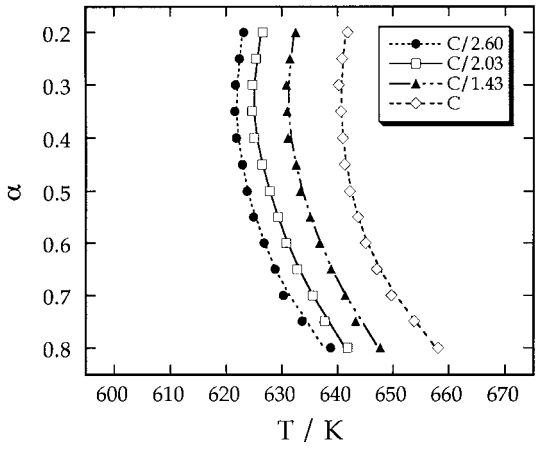

Fig. 11. Experimental α vs. *T* plots obtained by using different decomposition rates for the thermal decomposition of PET.

that the present analysis makes it possible to decrease the experimental dispersion.

A similar kinetic analysis was carried out for the thermal decomposition of PET. Fig. 11 shows the experimental α vs. *T* plots obtained by using relative different decomposition rates, i.e. *C*, *C*/1.43, *C*/2.03 and *C*/2.60, respectively. The circles indicate the *T* at $\Delta\alpha$=0.05 increments over the $0.2 \leq X \leq 0.8$ range. The results of analysis, according to Eq. (7), are shown in Fig. 12 and Table 3. A presumption regarding the reaction model is easy to specify in comparison to PBT, because a difference among the correlation coefficients between Fn and RSL types is considered significant. As a result, the RS2 or RS3 model was preferentially selected. However, both the correlation coefficients are close to 1.0 and are found to agree within experimental error. In this case, when the kinetic parameters are estimated with analysis accord-

Table 2
The pre-exponential factor results obtained from the representation of Eq. (12) using kinetic parameters of E=163 kJ mol^{-1} and RS2 model for the thermal decomposition of PBT.

X	*C*/2.23 (A×10^{12}/min^{-1})	*C*/1.79 (A×10^{12}/min^{-1})	*C*/1.22 (A×10^{12}/min^{-1})	*C* (A×10^{12}/min^{-1})
0.2	1.587	1.735	1.881	1.837
0.25	1.646	1.702	1.919	1.845
0.3	1.667	1.760	1.864	1.813
0.35	1.653	1.774	1.848	1.784
0.4	1.659	1.750	1.841	1.775
0.45	1.676	1.742	1.818	1.799
0.5	1.702	1.750	1.828	1.827
0.55	1.775	1.785	1.875	1.856
0.6	1.807	1.812	1.909	1.873
0.65	1.863	1.841	1.959	1.896
0.7	1.865	1.826	1.955	1.911
0.75	1.883	1.837	1.963	1.891
0.8	1.891	1.819	1.895	1.837
Mean	1.742	1.779	1.889	1.842
σ_n [a]	0.106	0.044	0.050	0.043

[a] Standard deviation.

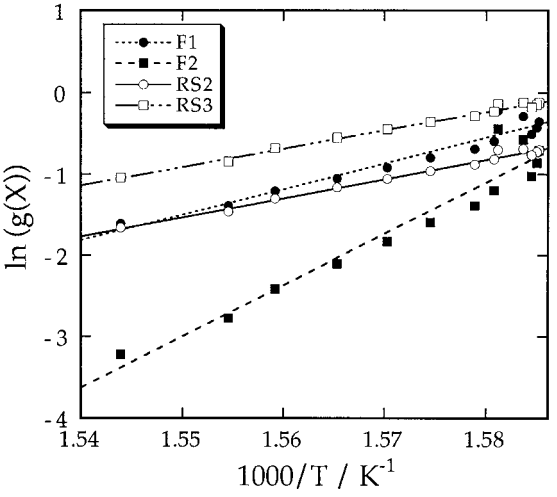

Fig. 12. Results obtained from the representation of Eq. (10) on assuming kinetic models of the Fn and RSL types in a single CDRC experiment.

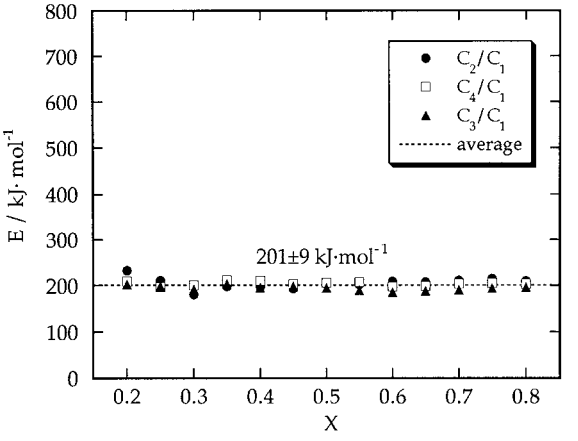

Fig. 13. Results obtained from the representaion of Eq. (12) by using each ratio of four decomposition rates. C_1, C/2.60; C_2, C/2.03; C_3, C/1.43; and C_4, C.

ing to Eq. (7), the magnitude of dispersion of the parameters obtained is a problem. As already mentioned, it is very difficult to determine the correct mechanism and to estimate the kinetic parameters on the basis of these representations.

Fig. 13 shows the results analyzed using each ratio of the different decomposition rates shown in Fig. 11 according to Eq. (10). The resulting mean activation energy, E, was estimated at 201 kJ mol^{-1}. As this figure indicated, the activation energy is independent of X over the range analyzed. Moreover, it follows from the listed values of the activation energy in Table 3 that the RS2 mechanism can be selected.

On the other hand, identification of the chemical species by means of the TG-MS method is based on molecular ion peak. The largest fragment ion observed was m/z 122 – the molecular ion peak of benzoic acid by analogy with the thermal decomposition of PBT.

Fig. 14 shows the plots of experimental data of X vs. ln [exp (E/RT)C] obtained at a decomposition rate of C/1.22 based on E=201 kJ mol^{-1}. It is superposed on the X vs. ln ($g(X)$) calculated by each kinetic model of

Table 3
Results obtained from the representation of e.g. [10] at four different decomposition rates for the thermal decomposition of PET.

Reaction rate	Mechanism symbol											
	F1			F2			RS2			RS3		
	r [a]	E [b]	$A\times10^{19}$ [c]	r [a]	E [b]	$A\times10^{40}$ [c]	r [a]	E [b]	$A\times10^{13}$ [c]	r [a]	E [b]	$A\times10^{10}$ [c]
C/2.60	0.9500	256	1.042	0.9500	513	5.403	0.9868	194	8.246	0.9891	185	8.185
C/2.03	0.9656	253	5.026	0.9655	505	0.983	0.9930	189	3.517	0.9941	180	3.508
C/1.43	0.9658	263	3.113	0.9658	526	26.42	0.9934	197	15.12	0.9944	188	14.33
C	0.9481	256	7.407	0.9481	512	0.876	0.9865	194	8.957	0.9890	185	9.412
Mean	0.9574	257	1.350	0.9574	514	8.421	0.9899	193.5	8.960	0.9916	184.5	8.859
σ_n [d]		4.2	2.715		8.8	12.18		3.3	4.764		3.3	4.448

[a] Correlation coefficient.
[b] Activation energy (kJ mol^{-1}).
[c] Pre-exponential factor (min^{-1}).
[d] Standard deviation.

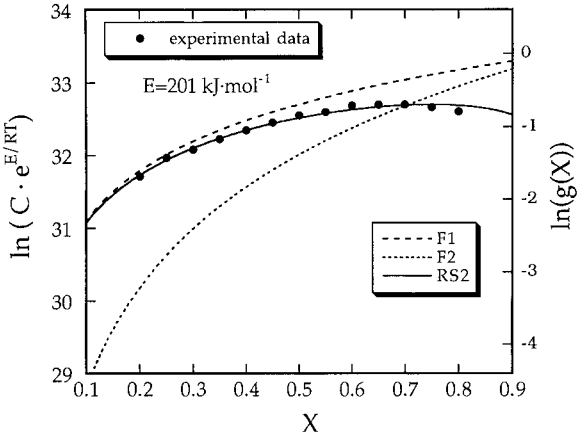

Fig. 14. Superimposition of experimental ln (*C*exp *E*/*RT*) vs. *X* and theoretical *g*(*X*) vs. *X* plot, in a single CDRC experiment.

F1, F2 and RS2. It is evident from Fig. 13 that the values observed agree very closely with the RS2 model curve. The pre-exponential factor estimated from an amount of the shift on the model curve at each decomposition rate is summarized in Table 4. The average pre-exponential factor, *A*, was estimated to be 3.213×10^{14} min^{-1}.

In conclusion, it must be borne in mind that any unknown gradient in the temperature, pressure and porous structure of the solid products cannot be specified in the conventional TA, and these unknown gradients are a real limit to our understanding of the kinetic phenomena. With the introduction of the CRTA method, uniform conditions exist throughout the sample by an appropriate control of the decomposition rate. In this respect, we can see that it is also to be the preferred method for measuring kinetic parameters. Simply examining the shape of the α vs. T curve, obtained in a CDRC method, was a quite efficient means to determine the reaction model. It is of great practical importance that there was a good correlation between the kinetic model obtained by CDRC analysis and the components observed by TG-MS.

On the basis of the above findings, it is concluded that CDRC (CRTA) offers significant advantages in this field of study, where we are dealing with thermal decomposition involving reaction models considering the assumption of a particular physical/chemical (e.g. kinetic) model. The controlled-rate thermogravimetric system utilizes the rate of mass loss directly as the object of control, so that the reaction rate maintains a precise constant value. It is expected that the CDRC and TG-MS techniques used in this study will be widely applicable to kinetic studies of the thermal decomposition of other polymers.

Table 4
The pre-exponential factors obtained from the representation of Eq. (12) using kinetic parameters of E=201 kJ mol^{-1} and RS2 model for the thermal decomposition of PET

X	*C*/2.60 ($A\times10^{14}$/min^{-1})	*C*/2.03 ($A\times10^{14}$/min^{-1})	*C*/1.43 ($A\times10^{14}$/min^{-1})	*C* ($A\times10^{14}$/min^{-1})
0.20	2.895	3.093	3.122	2.987
0.25	3.211	3.224	3.293	3.111
0.30	3.350	3.131	3.132	3.334
0.35	3.201	3.211	3.173	3.390
0.40	3.24	3.254	3.210	3.413
0.45	3.321	3.250	3.239	3.365
0.50	3.298	3.280	3.325	3.385
0.55	3.257	3.348	3.264	3.364
0.60	3.317	3.473	3.387	3.246
0.65	3.241	3.424	3.299	3.197
0.70	3.114	3.318	3.235	3.192
0.75	2.971	3.158	3.087	3.043
0.80	2.867	2.970	2.942	2.907
Mean	3.178	3.241	3.208	3.226
σ_n [a]	0.164	0.136	0.118	0.169

[a] Standard deviation.

References

[1] J. Rouquerol, J. Therm. Anal. 2 (1970) 123.
[2] J. Rouquerol, Thermochim. Acta 144 (1989) 209.
[3] O.T. Sorensen, Thermochim. Acta 138 (1989) 107.
[4] F. Paulik, J. Paulik, Thermochim. Acta 100 (1986) 23.
[5] J.M. Criado, F.J. Gotor, A. Ortega, C. Real, Thermochim. Acta 199 (1992) 235.
[6] F. Rouquerol, J. Rouquerol, G. Thevand, M. Triaca, Surface Sci. 162 (1985) 239.
[7] J.M. Creado, F.J. Gotor, C. Real, F. Jimenez, S. Ramos, J. Del Cerro, Ferroelectrics 115 (1991) 43.
[8] S. Bordere, F. Rouquerol, J. Rouquerol, J. Esfienne, A. Floreancig, J. Therm. Anal. 36 (1990) 1651.
[9] T. Arii, T. Kanaya, A. Kishi, N. Fujii, Netsu Sokutei 21 (1994) 151.
[10] T. Arii, T. Senda, N. Fujii, Thermochim. Acta 267 (1995) 209.
[11] T. Arii, A. Kishi, N. Fujii, Netsu Sokutei 23 (1996) 5.
[12] T. Arii, K. Terayama, N. Fujii, J. Therm. Anal. 47 (1996) 1649.
[13] T. Arii, N. Fujii, J. Anal. Appl. Pyrolysis 39 (1997) 129.
[14] S. Ichihara, N. Nakagawa, Y. Tsukazawa, Kobunshi Ronbunshu 51 (1994) 459.
[15] T. Ozawa, Bull. Chem. Soc. Japan 38 (1965) 1965.
[16] L.A. Wall, J.H. Fynn, Rubber Chem. Tech. 37 (1964) 937.
[17] R. Simha, L.A. Wall, J. Phys. Chem. 56 (1952) 707.